

Review

# Electrochemical Biosensors Based on Carbon Nanomaterials for Diagnosis of Human Respiratory Diseases

Chunmei Li, Bo Che and Linhong Deng \* 

Changzhou Key Laboratory of Respiratory Medical Engineering, Institute of Biomedical Engineering and Health Sciences, School of Medical and Health Engineering, Changzhou University, Changzhou 213164, China

\* Correspondence: dlh@cczu.edu.cn

**Abstract:** In recent years, respiratory diseases have increasingly become a global concern, largely due to the outbreak of Coronavirus Disease 2019 (COVID-19). This inevitably causes great attention to be given to the development of highly efficient and minimal or non-invasive methods for the diagnosis of respiratory diseases. And electrochemical biosensors based on carbon nanomaterials show great potential in fulfilling the requirement, not only because of the superior performance of electrochemical analysis, but also given the excellent properties of the carbon nanomaterials. In this paper, we review the most recent advances in research, development and applications of electrochemical biosensors based on the use of carbon nanomaterials for diagnosis of human respiratory diseases in the last 10 years. We first briefly introduce the characteristics of several common human respiratory diseases, including influenza, COVID-19, pulmonary fibrosis, tuberculosis and lung cancer. Then, we describe the working principles and fabrication of various electrochemical biosensors based on carbon nanomaterials used for diagnosis of these respiratory diseases. Finally, we summarize the advantages, challenges, and future perspectives for the currently available electrochemical biosensors based on carbon nanomaterials for detecting human respiratory diseases.

**Keywords:** electrochemical biosensors; respiratory diseases; carbon nanomaterials



**Citation:** Li, C.; Che, B.; Deng, L. Electrochemical Biosensors Based on Carbon Nanomaterials for Diagnosis of Human Respiratory Diseases. *Biosensors* **2023**, *13*, 12. <https://doi.org/10.3390/bios13010012>

Received: 8 November 2022

Revised: 13 December 2022

Accepted: 21 December 2022

Published: 22 December 2022



**Copyright:** © 2022 by the authors. Licensee MDPI, Basel, Switzerland. This article is an open access article distributed under the terms and conditions of the Creative Commons Attribution (CC BY) license (<https://creativecommons.org/licenses/by/4.0/>).

## 1. Introduction

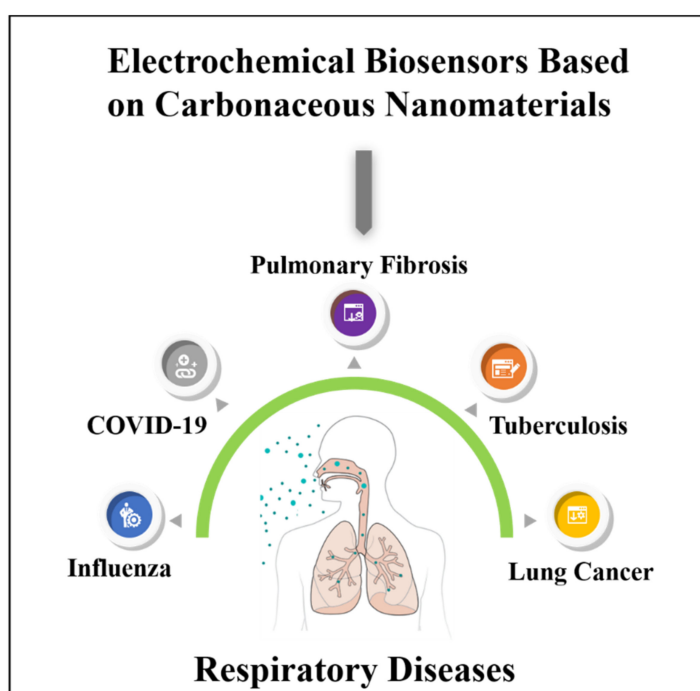
Respiratory diseases affect the nasal cavity, bronchi, lungs, chest and other parts of the human body, and can be either non-infectious, as in asthma, chronic obstructive pulmonary disease (COPD), chronic bronchitis and idiopathic pulmonary fibrosis, or infectious, as in pulmonary infections caused by viruses, bacteria and other microorganisms [1]. With the increasing extent of air pollution, smoking, aging population and other factors, respiratory diseases will also have an increasingly serious impact on the health of the people, as a result of increased incidence rate and mortality [2]. At present, respiratory diseases can be diagnosed with a variety of methods. For example, pulmonary fibrosis can be diagnosed by high-resolution computed tomography (HRCT) with high sensitivity [3]. And coronavirus disease 2019 (COVID-19) can be diagnosed by detection of SARS coronavirus 2 (SARS-CoV-2) using heterogeneous serological methods in the laboratory [4]. However, these methods are either time-consuming, expensive, or require further diagnostic examinations such as surgical lung biopsy and a multiple disciplinary consultation for diagnosis [5]. Therefore, it is urgent to develop simple, fast-operating diagnostic procedures for diagnosis of respiratory diseases in the early stage, such as those assisted by detection of respiratory viruses, related DNA fragments, proteins, or RNA with electrochemical biosensors.

The electrochemical biosensor is an important branch of the electrochemical sensor, which uses electrode as energy exchange element [6]. Compared with other types of sensors, the electrochemical biosensor is based on direct electronic signals, such as ampere, volt ampere and impedance changes [7,8]. The transduction process of electrochemical biosensors can be completed in a short space of time in the electrochemical workstation, greatly

reducing the test's time and cost [9–12]. In addition, the high sensitivity of electrochemical biosensors can be guaranteed by using biometric components with high specificity and affinity, or modifying electrodes with unique materials with distinctive electrical properties [9,13–15]. Electrochemical biosensors have been widely used in the field of analysis with their unique advantages, and have been especially used to detect respiratory viruses, related DNA fragments, proteins or RNA, to assist the diagnosis of respiratory diseases over recent years [16–24].

Carbon nanomaterials, less than 100 nm in size in at least one dimension, are composed of carbon atoms and non-carbon atoms, in which carbon atoms are commonly  $sp^2$  and  $sp^3$  hybridization [25]. These materials come in different forms including carbon quantum dots, graphene quantum dots, carbon nanotubes, graphene, graphitic carbon nitride (also known as  $g-C_3N_4$ ), fullerene and diamond [26]. They all have excellent physical, chemical, mechanical and electrical properties. In addition to good biocompatibility and bioactivity, carbon nanomaterials can be explored in one way or the other to fabricate biosensors [27]. Such biosensors have also shown great potential for diagnosis of respiratory diseases. For example, a biosensor fabricated with carbon nanotubes has been developed for diagnosis of lung cancer via the detection of long non-coding RNAs (lncRNAs), specifically, the biomarker metastasis-associated lung adenocarcinoma transcript 1 (MALAT1) in the blood [28]. And biosensors fabricated with carbon nanodots and graphene quantum dots have been demonstrated to be capable of detecting the presence of SARS-CoV-2, and Haemophilus influenza virus by monitoring of Haemophilus influenza genome in human plasma samples, respectively [29,30].

In this review, we will provide an overview of the most recent developments of electrochemical biosensors fabricated with carbon nanomaterials and their composites in the field of diagnosis of respiratory diseases (Scheme 1). We will focus on several common respiratory diseases, including influenza, pulmonary fibrosis, tuberculosis, lung cancer and COVID-19, in terms of their characteristics and diagnosis by using electrochemical biosensors based on carbon nanomaterials. Last but not least, we will briefly discuss the challenges and future perspectives of electrochemical biosensors based on carbon nanomaterials for the diagnosis of respiratory diseases.



**Scheme 1.** A summary of electrochemical biosensors based on carbon nanomaterials for detection of human respiratory diseases.

## 2. Characteristics of Carbon Nanomaterials and Human Common Respiratory Diseases

Carbon nanomaterials are materials less than 100 nm in size at least in one dimension. They are composed of carbon atoms and non-carbon atoms, in which carbon atoms are commonly  $sp^2$  and  $sp^3$  hybridization. Generally, they include carbon quantum dots, graphene quantum dots, carbon nanotubes, graphene, graphitic carbon nitride (also known as  $g-C_3N_4$ ), fullerene and diamond, and they all have excellent physical, chemical, mechanical and electrical properties. For more information related to carbon nanomaterials, please read a review I wrote earlier [25].

The respiratory system consists of the respiratory tract and lungs, wherein the respiratory tract consists of the nose, throat, larynx, trachea, bronchus and various bronchial branches in the lungs [31]. Respiratory diseases refer to the diseases in which lesions are located in the respiratory system. Common respiratory diseases include the infectious influenza, acute tracheobronchitis, chronic bronchitis, tuberculosis and COVID-19, and the non-infectious asthma, COPD, pulmonary fibrosis, lung cancer and so on [32–34]. Here we focus on influenza, COVID-19, pulmonary fibrosis, tuberculosis and lung cancer.

Influenza is an infectious acute respiratory disease caused by the influenza virus. Its clinical characteristics are acute infection, obvious symptoms, such as high fever, headache, systemic pain, weakness, etc. Influenza is mainly transmitted through contact and droplets [35]. It is highly infectious. There are various types of influenza viruses, including swine influenza virus, avian influenza virus, and influenza A, B, and C [36–41].

COVID-19 is another contagious respiratory disease, brought on by SARS-CoV-2, and first identified in 2019 [42]. SARS-CoV-2 is polymorphic or usually spherical, with a diameter range of 80–160 nm, and contains a single-positive strand RNA genome of about 30 kb with a 5' cap structure and a 3' poly(A) [43]. The 3' poly(A) tail of SARS-CoV-2 RNA genome can encode four main structural proteins, namely, spike (S) protein, envelope (E) protein, membrane (M) protein and nucleocapsid (N) protein [44]. When the S protein of SARS-CoV-2 binds to a person's cell's surface receptor, angiotensin converting enzyme 2 (ACE2), he will be infected [43,44]. SARS-CoV-2 transmits primarily through respiratory droplets by inhalation of sneezing, coughing, talking and exhaled droplets of gas. People who are infected may have typical symptoms, such as coughs or sneezes, or may not have symptoms [45]. In the process of transmission, the single-positive strand RNA genome of SARS-CoV-2 replicates continuously over time, and a variety of variants will appear. Currently, there are several SARS-CoV-2 variants, such as the Alpha, Beta, Gamma, Delta and Omicron variants [46,47]. Since December 2019, COVID-19 has greatly affected our lives and led to an unprecedented socio-economic burden.

Pulmonary fibrosis is a severe and long-lasting interstitial respiratory disease brought on by aggregation of fibroblasts and deposition of lung extracellular matrix, and more serious pulmonary fibrosis is commonly accompanied by malignant reaction and damage to the lung cells/tissue structure [48]. According to pathogenic factors, clinical presentation, relative responsiveness to immunosuppression and imaging characteristics, pulmonary fibrosis can be divided into primary pulmonary fibrosis, secondary pulmonary fibrosis, idiopathic pulmonary fibrosis, pulmonary interstitial fibrosis, interstitial pneumonia and pulmonary fibrosis caused by drugs or emission lines, and so on [20]. In recent years, pulmonary fibrosis, especially idiopathic pulmonary fibrosis, has affected millions of people and its incidence rate is rising year by year.

Tuberculosis is a chronic respiratory disease caused by a bacterium called *Mycobacterium tuberculosis* attacking the lungs [16–18]. In the initial stage, people with latently infected tuberculosis may only exhibit minor symptoms or none at all, and most early infections can only be found by X-ray examination [49]. When tuberculosis disease is serious, patients infected by *Mycobacterium tuberculosis* are hemoptysis, and then tuberculosis disease can be fatal if not treated properly [49]. Lung cancer is a disease in which lung cells proliferate out of control [50]. There are two main sub-type lung cancers, namely small cell lung cancer (including oat cell carcinoma, intermediate cell carcinoma and compound oat

cell carcinoma) or non-small cell lung cancer (including adenocarcinoma and squamous cell carcinoma), and the latter is more common than the former [51]. Lung cancer involves rapid proliferation and early extensive metastasis [22,23,52]. As a result, it may spread from one organ to another. For example, lung cancer may spread to lymph nodes or the brain. In comparison, cancer starting from other organs may also spread to the lungs [50]. The initial typical manifestation of lung cancer is cough and dyspnea caused by enlarged hilar mass and huge mediastinal lymph nodes, and it is more sensitive to radiotherapy and chemotherapy [50].

### 3. Electrochemical Biosensors Based on Carbon Nanomaterials for Diagnosis of Human Respiratory Diseases

Respiratory diseases often lead to dyspnea and shortness of breath in patients, which in turn leads to low blood oxygen saturation and gradual tissue hypoxia that can ultimately lead to coma and even death [31]. Once a human respiratory disease epidemic breaks out, there will inevitably be a shortage of medical personnel and equipment. At present, academic research efforts have focused on the treatment of acute large-scale epidemic respiratory diseases such as COVID-19 [53]. But the development of advanced routine diagnostic methods for respiratory diseases is still of great significance for the demand for early accurate detection of the diseases.

Currently widely-used routine diagnostic methods such as chest X-ray, polymerase chain reaction (PCR) detection, Xpert MTB/RIF and immunological detection [54,55] are defective in speed for analysis, sensitivity, discriminatory power and specificity. In contrast, electrochemical biosensors are known to be advantageous in simplicity, speed, sensitivity, and low operation cost, which makes them potential alternative tools for routine diagnosis of human respiratory diseases and recently has received great attention from the research community [6,17–19,37,56].

Furthermore, carbon nanomaterials have proved to be superior for fabrication of electrochemical biosensors. By definition, carbon nanomaterials are carbon-based materials composed of  $sp^2$  and  $sp^3$ -bonded carbon atoms or heterogeneous components (non-carbon atoms) with at least one dimension of less than 100 nm [25]. These materials come in different forms, including carbon quantum dots, graphene quantum dots, carbon nanotubes, graphene, graphitic carbon nitride (also known as  $g-C_3N_4$ ), fullerene and diamond. But they all have exceptional physicochemical and biological qualities. For example, carbon quantum dots or graphene quantum dots are well-known for their small diameters ( $\sim 5$  nm), chemical inertness, minimal toxicity, superior biocompatibility and photoluminescent stability [57,58]. On the other hand, carbon nanotubes can provide a relatively large surface area with unique physical and chemical properties and surface functionalization ability. Graphene or graphene oxide is known for its superior water solubility, in addition to a huge surface area with distinctive surface properties and minimal cytotoxicity [59]. Further,  $g-C_3N_4$  (bulk, nanosheets, and quantum dots) possesses exceptional optical qualities, chemical and thermal stability together with biocompatibility and minimal toxicity [60]. Fullerene is a common zero-dimensional carbon material associated with large conductivity and strong electron receptivity as well as unique redox activity [20,61]. And in addition to good biocompatibility and bioactivity, diamond has been reported to have excellent fluorescent capacity, and a cost-effective advantage for large-scale manufacturing of medical devices [62,63]. These superior properties of carbon nanomaterials can be explored in one way or the other to fabricate tailor-made electrochemical biosensors for diagnosis of various human respiratory diseases.

Currently, a series of electrochemical biosensors based on carbon nanomaterials have been developed and widely used for the diagnosis of respiratory diseases, demonstrating their great potential in clinical applications. For example, as COVID-19 broke out in 2019, electrochemical biosensors fabricated with graphene oxide that had been functionalized to target specific RNA of SARS-CoV-2 were used for the diagnosis of COVID-19 [64]. For diagnosis of lung cancer, electrochemical biosensors were fabricated with three-dimensional

(3D) graphene to identify two lung cancer biomarkers, cytokeratin 19 fragment 21-1 and carcinoembryonic antigen [65]. In addition, multi-walled carbon nanotubes have been used to develop an electrochemical DNA biosensor to detect *Mycobacterium tuberculosis* bacteria for the diagnosis of tuberculosis. More details of these electrochemical biosensors based on carbon nanomaterials will be described and discussed respectively in the following.

### 3.1. Electrochemical Biosensors for Influenza Diagnosis

Influenza viruses, including influenza A, B, and C viruses as well as the swine and avian influenza viruses, have become an increasingly serious hazard to human health. Every year, especially in the winter, a large number of people are infected by influenza virus via its directly crossing the human immune barriers. Obviously, effective methods for detecting the presence of the highly infectious influenza virus are urgently needed for monitoring and controlling the spread of viral infection among the population. Electrochemical methods have proven to be excellent alternative options for detecting influenza virus, with antibodies or nucleic acid as recognition reagents [66–68]. Recently, carbon nanomaterials have been used to fabricate electrochemical biosensors for detection of Haemophilus influenza, influenza A virus (such as H1N1, H5N1 and H7N9 influenza A virus), avian influenza virus (such as H5N1, H7N9, and H9N2) and swine influenza virus (such as H1N1 swine influenza virus) [30,36,41,69,70].

Specifically, Anik et al. have developed an influenza A biosensor that used an Au-screen printed electrode modified with graphene gold hybrid nanocomposite for an electrochemical impedance spectroscopy (EIS) analysis and demonstrated these biosensors for successful detection of the real influenza virus A (H9N2), as shown in Figure 1a [71]. Reddy et al. have developed influenza biosensors using a nickel oxide (NiO)-reduced graphene oxide (rGO)/MXene nanocomposite for detection of both active influenza viruses (H1N1 and H5N2) and influenza proteins via electrochemical signals (Figure 1b) [70].

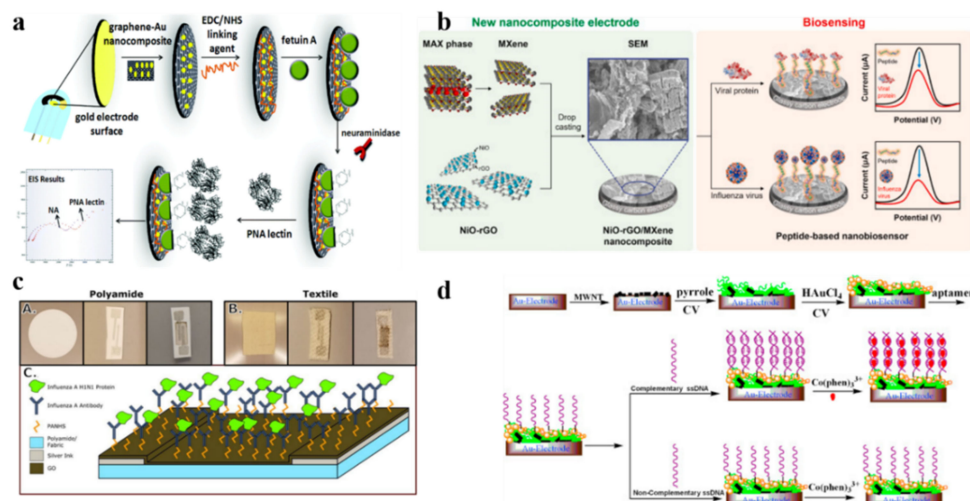


**Figure 1.** Schematic diagram depicting fabrication of electrochemical biosensors with carbon nanomaterials for detecting influenza: (a) biosensor fabricated with graphene for detecting influenza A [71]; (b) biosensor fabricated with a nickel oxide-reduced graphene oxide (NiO-rGO)/MXene nanocomposite for detecting influenza virus and viral protein [70]; (c) biosensor fabricated with graphene oxide layer supported by both nanoporous polyamide and consumer utility textiles for detecting environmental exposure to influenza A virus [39]; (d) biosensor fabricated with multi-wall carbon nanotubes for detection of H5N1 gene sequence of avian influenza virus [37]. (a) Reproduced with permission Copyright 2017, Royal Society of Chemistry. (b,d) Reproduced with permission Copyright 2022, 2011, Elsevier B.V. (c) Reproduced with permission Copyright 2018, ECS.

Kinnamon et al. have fabricated a textile screen-printed influenza electrochemical biosensor for detecting influenza A virus exposed to the environment, using graphene oxide as transduction film of the textile screen-printed electrode (Figure 1c) [39]. Interestingly, Liu et al. have developed an electrochemical biosensor for detecting H5N1 gene sequence of avian influenza virus (AIV), in which multi-wall carbon nanotubes (MWNT), together with polypyrrole nanowires (PPNWs) and gold nanoparticles (GNPs), was used to fabricate a hybrid nanomaterial-modified electrode for immobilized DNA aptamer (Figure 1d) [37].

These electrochemical biosensors based on carbon nanomaterials for diagnosis of influenza described above have excellent performance, and details are shown in Table 1.

**Table 1.** Performances of electrochemical biosensors for influenza diagnosis.

Carbon Nanomaterials	Mechanism of Detection	Target	Analytical Performances (LOD = Limit of Detection, R <sup>2</sup> Refers to Determination Coefficient, Relative Standard Deviation Value = RSD)	Ref.
Graphene gold hybrid nanocomposite	EIS	Neuraminidase (a surface glycoproteins of H9N2 influenza virus A) activity	Linear range: 10 <sup>-8</sup> U/mL~10 <sup>-1</sup> U/mL with RSD 3.23%; LOD: 10 <sup>-8</sup> U/mL; Real sample analysis: detecting real H9N2 influenza type A virus with sensitivity and accuracy compared with the ELISA assay results	[71]
Reduced graphene oxide	Cyclic voltammetry (CV)	Surface protein hemagglutinin of H5N1 and H1N1 influenza virus	Linear range: 25~300 nM; LOD: 2.29 nM in PBS and 2.39 nM in human blood plasma for H5N1, LOD: 3.09 nM in PBS and 3.63 nM in human blood plasma for H1N1; Real sample analysis: accuracy for real analysis with percentage of recoveries 89~101% for H5N1 and 86~103% for H1N1 via recovery studies by spiking human plasma with different concentrations of hemagglutinin of H5N1 and H1N1; Stability and selectivity	[70]
graphene oxide	EIS	H1N1 Influenza A protein	Linear range: 0 ng/mL~10 µg/mL; LOD: 10 ng/mL; Stability and repeatability	[39]
Multi-wall carbon nanotubes	Differential pulse voltammetry (DPV)	Avian influenza virus H5N1 gene sequence	Linear range: 5.0 × 10 <sup>-12</sup> ~1.0 × 10 <sup>-9</sup> M (R <sup>2</sup> = 0.9863); LOD: 4.3 × 10 <sup>-13</sup> M; High recognition and selectivity for H5N1 specific sequence	[37]

### 3.2. Electrochemical Biosensors for COVID-19 Diagnosis

The pandemic of COVID-19 brought on by SARS CoV-2 may become more serious under evolutionary pressure due to the emergence of transmissibility, pathogenicity and pathogenicity or SARS CoV-2 variants (such as Alpha, Beta, Gamma, Delta variant or Omicron variant) [72]. Additionally, SARS CoV-2 may become more adaptable and develop into a runaway form due to antibodies in COVID-19 convalescence or vaccine recipients. Traditional SARS CoV-2 detection methods mostly rely on laboratory technology, specifically, from initial virus culture, morphological observation and serological test to subsequent reverse transcription PCR, isothermal amplification technology, immunochromatography, and enzyme-linked immunosorbent immunofluorescence assay [73,74]. In comparison, the electrochemical biosensor is faster, more sensitive and accurate to identify and quantify SARS CoV-2, and therefore has become one of the most rapidly developing area in the field.

So far, it has been reported that a variety of COVID-19 electrochemical biosensors have been based on carbon nanomaterials [75]. The carbon nanomaterials used to fabricate electrochemical biosensors include, but are not limited to, graphene, graphene oxide nanocolloids, boron-doped diamond and functionalized graphene oxide [42,47,76]. And it has also been demonstrated that the electrochemical biosensors based on carbon nanomaterials could be used to successfully detect a DNA sequence corresponding to SARS-CoV-2, a SARS-CoV-2 nucleocapsid protein, a RNA of SARS-CoV-2, a protein sequence of the N protein of SARS-CoV-2, a SARS-CoV-2 spike protein, a SARS-CoV-2 S1 antigen, and SARS-CoV-2 variant Delta and a SARS-CoV-2 S protein, and so on [29,62,64], [77,78].

Figures 2 and 3 show the design of some of these biosensors and the procedure for detecting SARS-CoV-2. In the first case, Ramanathan et al. have exploited a portable electrochemical biosensor for detecting SARS-CoV-2 nucleocapsid protein (NCP) as diagnosis of COVID-19, which used a gap-sized gold interdigitated electrode (AuIDE) deposited with ~20 nm diamond (Figure 2a) [62]. In the second case, Beduk et al. have developed a point-of-care (POC) COVID-19 diagnostic, in which a laser-scribed graphene (LSG)-based biosensing platform was built based on a miniaturized electrochemical sensing scheme combined with 3D gold nanostructures (Figure 2b) [46]. In the third case, Zhao et al. developed a portable electrochemical smartphone system for remote diagnosis of COVID-19, in which an electrochemical biosensor was fabricated with calixarene functionalized graphene oxide based on a super-sandwich-type recognition strategy, wherein calixarene functionalized graphene oxide was used to target RNA of SARS-CoV-2. The electrochemical biosensor has been confirmed to effectively detect the RNA of SARS-CoV-2 in the absence PCR and reverse-transcription process (Figure 3a) [64]. In the fourth case, Zamzami et al. have developed an electrochemical biosensor based on carbon nanotube field-effect transistor (CNT-FET) for detecting a SARS-CoV-2 S1 antigens in saliva samples, and this detection has been shown to be fast (2–3 min), quantitative, easy to use, and at a low cost (Figure 3b) [79].

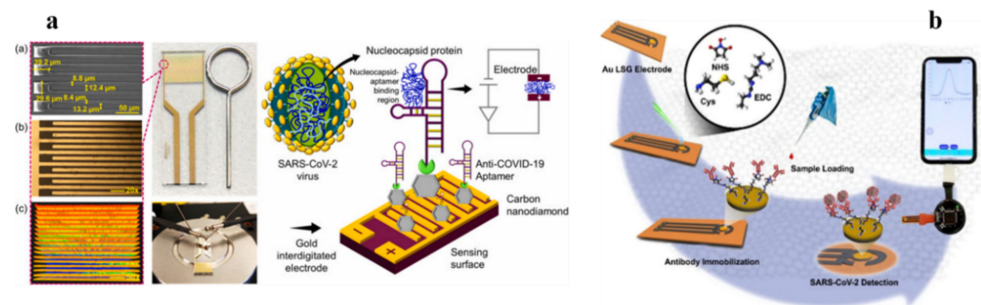


**Figure 2.** Schematic illustration of electrochemical biosensors fabricated with carbon nanomaterials for detection of SARS-CoV-2: (a) biosensor based on anti-NCP aptamer on diamond enhanced gold interdigitated electrode (AuIDE) for detecting NCP of SARS-CoV-2 [62]; (b) biosensor based on gold-nanoarchitecture-assisted laser-scribed graphene for detecting SARS-CoV-2 at the point-of-care [46]. Note: (a) is reproduced with permission Copyright 2021, Elsevier B.V.; (b) is reproduced with permission Copyright 2021, American Chemical Society.

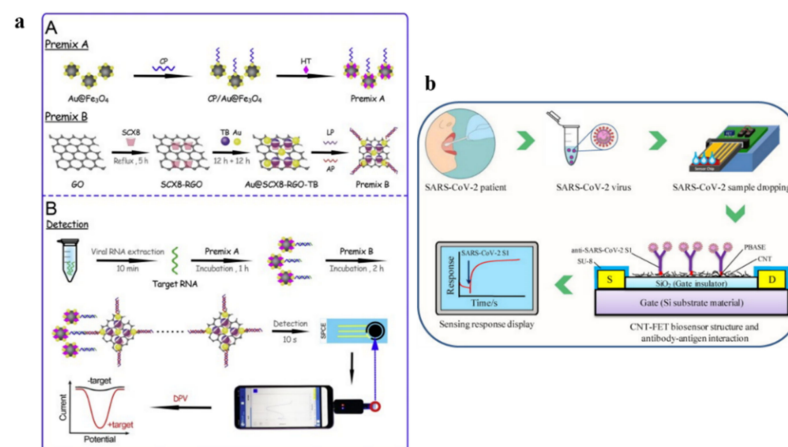


**Figure 3.** Schematic illustration of electrochemical biosensors fabricated with carbon nanomaterials for detection of SARS-CoV-2: (a) biosensor based on graphene oxide with calixarene functionality for detecting RNA of SARS-CoV-2 via a smartphone [64]; (b) biosensor based on CNT-FET for detecting SARS-CoV-2 S1 antigens [79]. Note: (a,b) are reproduced with permission Copyright 2021, Elsevier B.V.

These electrochemical biosensors based on carbon nanomaterials for diagnosis of COVID-19 described above have excellent performance; the details are shown in Table 2.

**Table 2.** Performances of electrochemical biosensors for COVID-19 diagnosis.

Carbon Nanomaterials	Mechanism of Detection	Target	Analytical Performances	Ref.
~20 nm diamond	EIS	SARS-CoV-2 nucleocapsid protein	Linear range: 1 fM~100 pM. ( $R^2 = 0.9863$ ); LOD: 0.389 fM; Selectivity, specificity, stability and reusability	[62]
Laser-scribed graphene (LSG)	DPV	SARS-CoV-2 S1 spike protein	Linear range: 5.0~500 ng/mL. ( $R^2 = 0.996$ ); LOD: 2.9 ng/mL; Real sample analysis: successful COVID-19 diagnosis carried out on 23 patient blood serum samples; User-friendly diagnostic platform; Ease of operation; Accessibility and systematic data management; Faster results compared to commercial diagnostic tools	[46]
Calixarene functionalized graphene oxide	DPV	RNA of SARS-CoV-2	Linear range: 5.0~500 ng/mL. ( $R^2 = 0.945$ ); LOD: 3 aM; Real sample analysis: higher detectable ratios (85.5 % and 46.2 %) than those obtained using RT-qPCR (56.5 % and 7.7 %); High specificity and selectivity; Only two copies (10 $\mu$ L) of SARS-CoV-2 were required for per assay	[64]
Carbon nanotube	Field-effect transistor (FET) technology	SARS-CoV-2 S1 antigen	Linear range: 0.1~5000 fg/mL; LOD: 4.12 fg/mL; Good selectivity to SARS-CoV-2 S1, Able to discriminate SARS-CoV-2 S1, SARS-CoV-1 S1 and MERS-CoV S1 antigens; Rapidly testing people for SARS-CoV2 infection; Easy to handle	[79]

### 3.3. Electrochemical Biosensors for Pulmonary Fibrosis Diagnosis

Pulmonary fibrosis is a severe chronic and progressive interstitial respiratory disease, and it has typical clinical symptoms such as dyspnea and dry cough. At present, high-resolution computed tomography (HRCT) is extensively used for the screening diagnosis of pulmonary fibrosis, which is highly sensitive. However, some patients do not show typical HRCT features and require further diagnostic examinations with surgical lung biopsy. The procedure of surgical lung biopsy is invasive and causes great pain to the patient. Therefore, it is desirable to develop alternative non-/minimal invasive procedures to assist in the diagnosis of pulmonary fibrosis. Electrochemical biosensors based on carbon nanomaterials have appeared to meet this requirement by detecting biomarkers of pulmonary fibrosis. For example, Zuo et al., have proposed an electrochemical biosensor using fullerene (C60) as electrode materials for detecting miR-3675-3p in human serum, which is known as a promising biomarker for pulmonary fibrosis [20]. Electrochemical biosensors based on a carbon-nanodots-modified screen-printed gold electrode as a transducer for gene detection, or based on carbon nanofibers for protein detection of cystic fibrosis transmembrane regulator (CFTR) as a biomarker of pulmonary fibrosis, have been reported, respectively [80,81]. Bonanni et al., have reported an electrochemical biosensor for diagnosis of pulmonary fibrosis, one based on gold nanoparticles in a graphite-epoxy nanocomposite (nanoAu-GEC) for the detection of triple base mutation deletion in a human DNA sequence related cystic-fibrosis [48].

These electrochemical biosensors based on carbon nanomaterials for diagnosis of pulmonary fibrosis described above have excellent performance, and the details are shown in Table 3.

**Table 3.** Performances of electrochemical biosensors for fibrosis diagnosis.

Carbon Nanomaterials	Mechanism of Detection	Target	Analytical Performances (S/N refers to a Signal to Noise Ratio)	Ref.
Fullerene	DPV	Biomarker miR-3675-3p for idiopathic pulmonary fibrosis	Linear range: 10 fM~10 nM ( $R^2 = 0.9976$ ); LOD: 2.99 fM calculated with $M + 3\delta$ (M: the average of DPV signal response; $\delta$ : the standard deviation of blank solution); Outstanding reproducibility and specificity; Good recovery (from 94.2% to 103.7%) in the spiked serum	[20]
Carbon nanodots	DPV	F508del mutation in the cystic fibrosis transmembrane regulator gene	Linear range: 0.001~20 $\mu$ M ( $R^2 = 0.998$ ); LOD: 0.16 nM; High reproducibility and selectivity	[80]
Carbon nanofiber	Square wave voltammograms (SWV)	Survival motor neuron 1	Linear range: 1 pg/mL~1 $\mu$ g/mL ( $R^2 = 0.981$ ); LOD: 0.74 pg/mL	Multiplexed immunosensor; Strong selectivity against non-specific proteins; High recovery percentage in spiked whole blood samples
		Cystic fibrosis transmembrane conductance regulator (CFTR)	Linear range: 1 pg/mL~1 $\mu$ g/mL ( $R^2 = 0.989$ ); LOD: 0.9 pg/mL	
		Duchenne muscular dystrophy proteins	Linear range: 1 pg/mL~10 ng/mL ( $R^2 = 0.979$ ); LOD: 0.7 pg/mL	
Gold nanoparticles graphite-epoxy nanocomposite	EIS	Triple base mutation deletion in a cystic-fibrosis	Linear range: 0.3 fmol~30 pmol; LOD: 22.5 (S/N = 3)	[48]

### 3.4. Electrochemical Biosensors for Tuberculosis Diagnosis

Tuberculosis is a global public health concern, as one of the top 10 causes of death in the world. Therefore, it is crucial to have high-quality diagnosis of the disease. Conventional methods of diagnosis include culture-based/culture-independent methods, imaging-based methods, antigen detection, serological tests, PCR assay and so on, which all aim to identify the presence of *Mycobacterium tuberculosis* directly or indirectly [82,83]. But these conventional methods are known for limitations in terms of sensitivity, specificity, delayed response time, need for skilled personnel and expensive instrumentation [84–87]. In comparison, tuberculosis detection methods based on electrochemical biosensors would have the advantages of cost effectiveness, detection speed and accuracy, as well as excellent biological and chemical properties if the biosensors are fabricated with carbon nanomaterials. Therefore, a variety of electrochemical biosensors have been recently reported for the detection of *Mycobacterium tuberculosis* or its biomarkers [84,88,89]. These biosensors have mainly been fabricated with carbon nanomaterials, including graphene oxide nanoribbons [16], carbon nanotubes [18], fullerene nanoparticles [19], graphene oxide [90], 3D graphene [91], graphene quantum dot [92], and nitrogen-doped carbon nanodots [93]. For tuberculosis detection, these biosensors generally detected *Mycobacterium tuberculosis* [90], while some detected biomarkers of *Mycobacterium tuberculosis* such as CFP10-ESAT6 antigen and ESAT-6 antigen [86,92,94], *Mycobacterium tuberculosis* DNA sequence [17,18,91], interferon gamma (IFN- $\gamma$ ) [95] and methyl nicotinate (metabolite of *Mycobacterium tuberculosis*) [96] and so on.

Figures 4 and 5 further illustrate the design of some of these electrochemical biosensors based on carbon nanomaterials and the procedures used for detecting *Mycobacterium tuberculosis* or its biomarkers. The first is an electrochemiluminescence (ECL) biosensor fabricated with self-enhanced ruthenium (Ru) II-based nanocomposite (NCNDs-BPEI-Ru) which has proved to be ultrasensitive for detection of *Mycobacterium tuberculosis* (Figure 4a) [93]. The NCNDs-BPEI-Ru nanocomposite was synthesized using nitrogen-doped carbon nanodots (NCNDs), tris (4,4'-dicarboxylic acid-2,2'-bipyridyl) Ru II dichloride ( $\text{Ru}(\text{dcbpy})_3\text{Cl}_2$ ),

polyethyleneimine (BPEI). The second is another ECL biosensor fabricated with gold nanoparticle-coated magnetic beads (AuNP@MB), and the AuNP@MB was attached on a nanofiber prepared using graphene oxide and polyaniline, namely GO-PANI-NF. The ECL biosensor proved to be a very sensitive, real-time and dynamic sensor for detecting IFN- $\gamma$  in blood as a biomarker for latent infection of *Mycobacterium tuberculosis* (Figure 4b) [95]. The third is a universal amperometric DNA biosensor fabricated with carbon nanotubes doped with polyaniline (CNTs-PAN) nano hybrid. The CNTs-PAN nano hybrid was a flower-like structure which can provide a large surface area with abundant active groups and efficient redox activity to form a tracer label. The flower-like CNTs-PAN nano hybrid can generate and amplify the electrochemical signal, resulting in ultra-sensitive detection of the specific IS6110 DNA sequence of *Mycobacterium tuberculosis* (Figure 5a) [18]. The last is an electrochemical biosensor fabricated with gold nanoparticles (AuNPs) immobilized over reduced graphene oxide nanoribbons (RGONRs), which was developed for detecting target *Mycobacterium tuberculosis* (Figure 5b) [16].

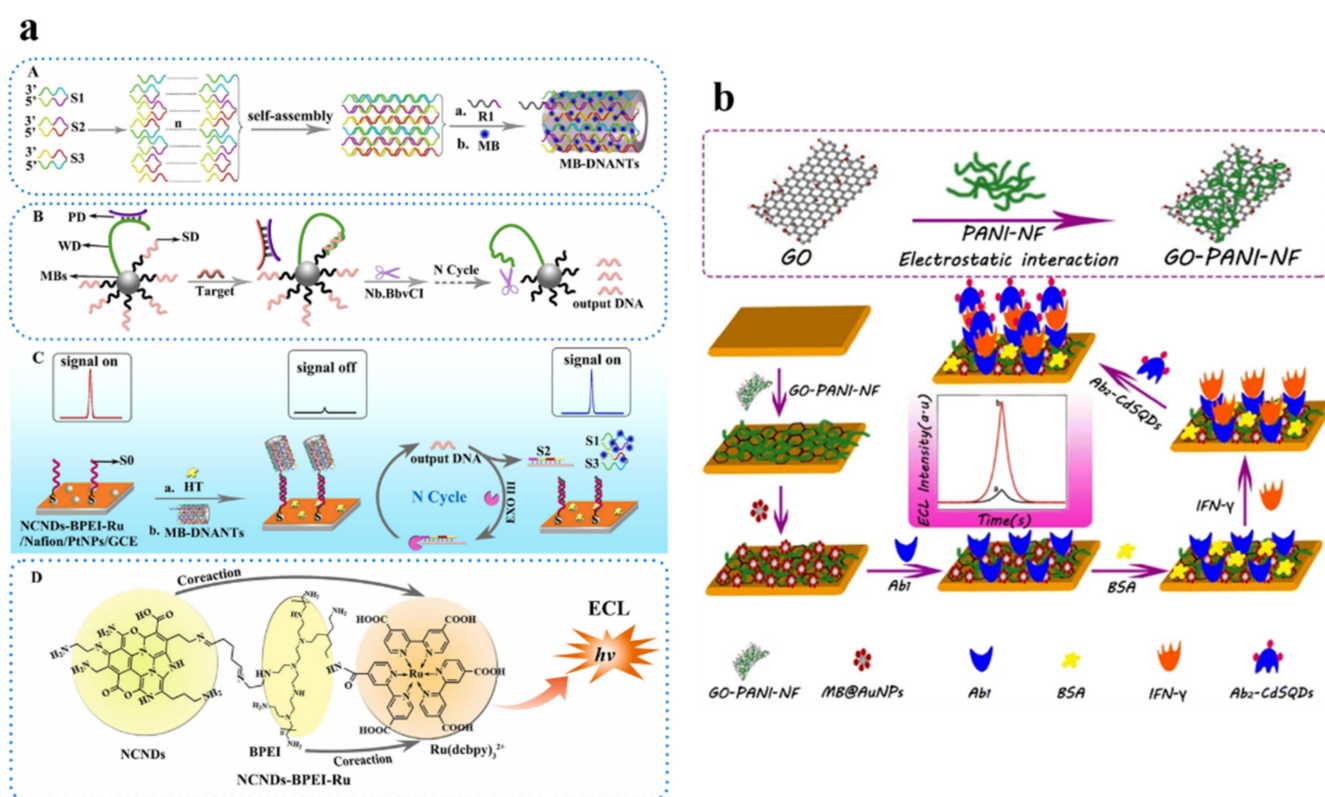


**Figure 4.** Schematic illustration of electrochemical biosensors fabricated with carbon nanomaterials for detection of *Mycobacterium tuberculosis*: (a) biosensors fabricated with self-assembled DNA nanotubes embedded with methylene blue molecules (MB-DNANTs) and NCNDs-BPEI-Ru for detection of *Mycobacterium tuberculosis* [93]; (b) biosensor fabricated with gold nanoparticle-coated magnetic beads (AuNP@MB) attached on a nanofiber prepared from graphene oxide and polyaniline (GO-PANI-NF) for detection of IFN- $\gamma$  related to latent infection of *Mycobacterium tuberculosis* [95]. (a) reproduced with permission Copyright 2021, Elsevier B.V. (b) Reproduced with permission Copyright 2016, Springer-Verlag Wien.

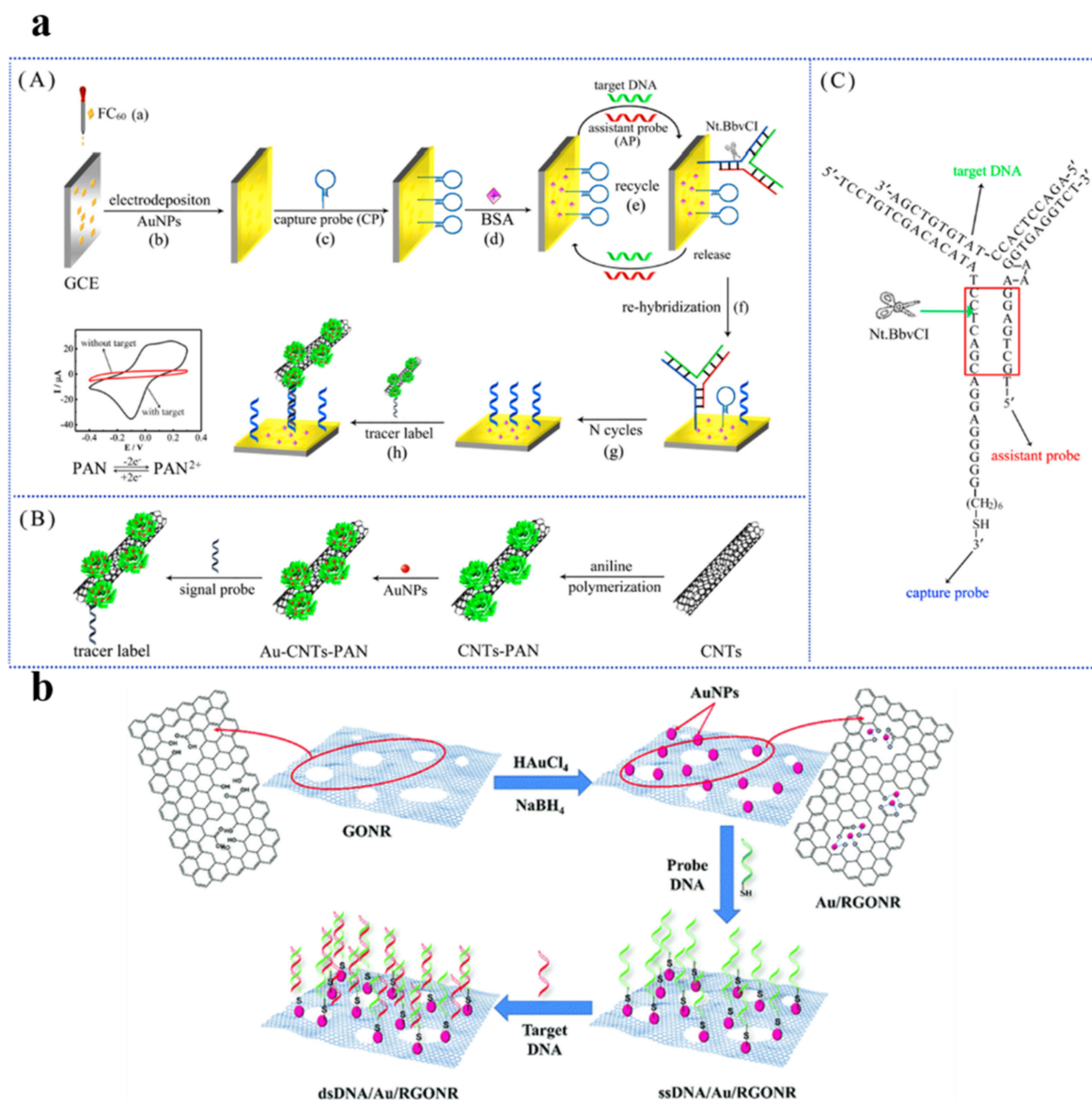


**Figure 5.** Schematic illustration of electrochemical biosensors fabricated with carbon nanomaterials for detection of *Mycobacterium tuberculosis*: (a) biosensor fabricated with carbon nanotubes doped with flower-like polyaniline (CNTs-PAN) nano hybrid structure and Y-shaped three-way DNA junction structure for detection of the specific IS6110 DNA sequence of *Mycobacterium tuberculosis* [18]; (b) biosensor fabricated with gold nanoparticles (AuNPs) immobilized over reduced graphene oxide nanoribbons (RGONRs) for detecting target *Mycobacterium tuberculosis* [16]. (a) reproduced with permission Copyright 2018 Elsevier B.V. (b) Reproduced with permission Copyright 2018, Royal Society of Chemistry.

These electrochemical biosensors based on carbon nanomaterials for diagnosis of tuberculosis described above have excellent performance, and details are shown in Table 4.

### 3.5. Electrochemical Biosensors for Lung Cancer Diagnosis

Lung cancer has been a major concern worldwide due to the highest morbidity and mortality rate associated with the disease. Therefore, the development of adequate techniques for detecting lung cancer biomarkers is urgently required for close monitoring of the patients. And several electrochemical biosensors based on carbon nanomaterials have shown great potential in this regard.

**Table 4.** Performances of electrochemical biosensors for tuberculosis diagnosis.

Carbon Nanomaterials	Mechanism of Detection	Target	Analytical Performances	Ref.
Nitrogen-doped carbon nanodots (NCNDs)	ECL	<i>Mycobacterium tuberculosis</i> DNA fragment	Linear range: 50 aM~1 nM. ( $R^2 = 0.9974$ ); LOD: 1.4 aM; Specificity and stability	[93]
Graphene oxide	ECL	Interferon gamma (IFN- $\gamma$ )	Linear range: 0.1~500 pg·mL <sup>-1</sup> ( $R^2 = 0.9913$ ); LOD: 30 fg·mL <sup>-1</sup> ; Real sample analysis: capacity for determining IFN- $\gamma$ in real biological samples with 96~103% recoveries; Successfully used for sensitive monitoring IFN- $\gamma$ levels in peripheral blood mononuclear cell	[95]
Tufted carbon nanotubes (CNTs)	DPV	Specific IS6110 DNA sequence of <i>Mycobacterium tuberculosis</i>	Linear range: 1 fM~10 nM ( $R^2 = 0.9910$ ); LOD: 0.33 fM (S/N = 3); Real sample analysis: High specificity and sensitivity for <i>Mycobacterium tuberculosis</i> detection in clinical samples	[18]
Reduced graphene oxide nanoribbon	CV	target DNA of <i>Mycobacterium tuberculosis</i>	Linear range: 0.1 fM~10 <sup>-6</sup> M; High detection efficiency (0.1 fM); Excellent specificity (92%) to <i>Mycobacterium tuberculosis</i> target DNA	[16]

As shown in Figure 6a, Zhuo et al., have developed a novel immuno-electrochemical biosensor for sensitive detecting a specific small cell lung cancer (SCLC) biomarker, progastrin releasing-peptide (ProGRP). The electrode of the biosensor was fabricated with Au nanoparticle/graphene together with ferrocene and glucose oxidase-multifunctional Au/TiO<sub>2</sub> nanocomposites, in which Au nanoparticle/graphene served as an antibody immobilization matrix [52]. On the other hand, Chen et al. have developed a transistor-based electrochemical biosensor for sensitively and conveniently detecting sialic acid level in serum samples. Sialic acid residues are generally highly expressed by cancer cells, which can be used as lung cancer biomarker. The transistor-based electrochemical biosensor consisted of three standard electrodes. One of the electrodes was modified with carboxylated multi-wall carbon nanotubes, which can produce the drain-source channel current signal; therefore, sialic acid in serum samples can be sensitively detected (Figure 6b) [97].

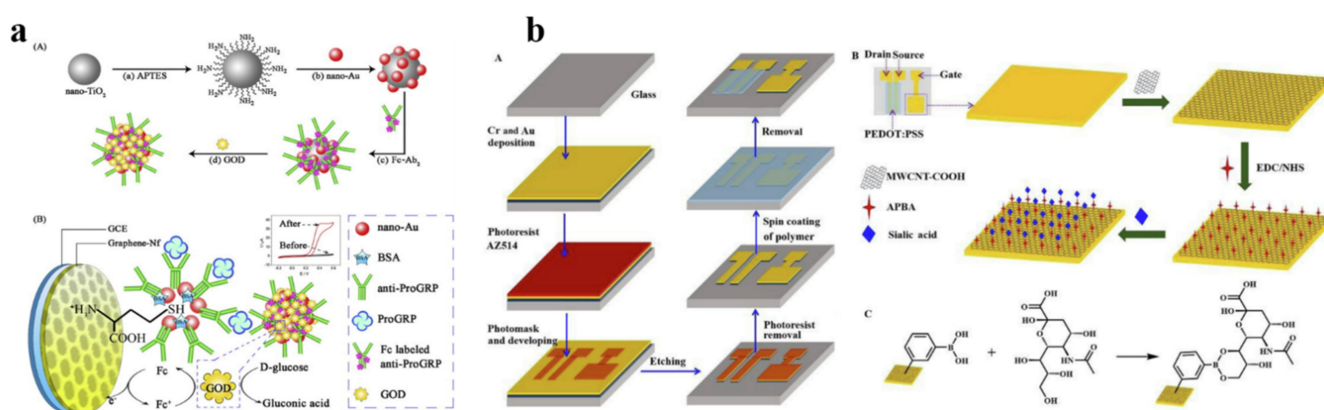


**Figure 6.** Schematic illustration of electrochemical biosensors fabricated with carbon nanomaterials for detection of lung cancer: (a) biosensor fabricated with ferrocene labeled secondary antibodies (Fc-Ab<sub>2</sub>) and glucose oxidase (GOD) multi-labeled nano-Au/TiO<sub>2</sub> nanospheres for detection of ProGRP, a biomarker of small cell lung cancer [52]; (b) biosensor fabricated with organic electrochemical transistor (OECT) for detecting lung cancer related sialic acid [97]. (a) and (b) Reproduced with permission Copyright 2011, 2020, Elsevier B.V.

Furthermore, Jafari-Kashi et al. have designed a label-free electrochemical DNA-biosensor for the early diagnosis of lung cancer via the detection of lung cancer biomarker, cytokeratin 19 fragment 21-1 (CYFRA21-1). The biosensor electrode was modified with reduced-graphene oxide, poly pyrrole, silver nanoparticles and single-strand DNA for capture of the lung cancer biomarker (Figure 7a) [24]. Similarly, Choudhary et al. used carbon nanotubes and chitosan (CNT-CHI) composite to develop a label-free electrochemical immunosensor for simultaneously detecting anti-MAGE A2 and anti-MAGE A11, which are also known biomarkers of lung cancer (Figure 7b) [51].

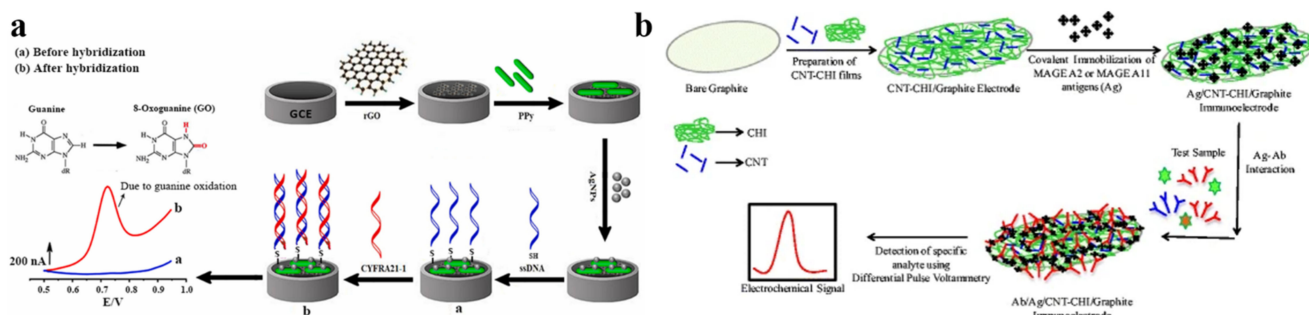


**Figure 7.** Schematic illustration of electrochemical biosensors fabricated with carbon nanomaterials for detection of lung cancer: (a) biosensor fabricated with reduced-graphene oxide together with poly pyrrole, silver nanoparticles and single-strand DNA for identifying lung cancer biomarker, CYFRA21-1 [24]; (b) biosensor fabricated with CNT-CHI composite for identifying lung cancer biomarkers, anti-MAGE A2 and anti-MAGE A11 [51]. (a) Reproduced with permission Copyright 2022, Elsevier B.V. (b) Reproduced with permission Copyright 2014, Springer-Verlag Wien.

These electrochemical biosensors based on carbon nanomaterials for diagnosis of lung cancer described above have excellent performance; details are shown in Table 5.

**Table 5.** Performance of electrochemical biosensors for lung cancer diagnosis.

Carbon Nanomaterials	Mechanism of Detection	Target	Analytical Performances	Ref.
Nano-Au functionalized graphene sheets	CV	Progastrin releasing-peptide (ProGRP)	Linear range: 10.0~500 pg/mL, ( $R^2 = 0.996$ ); LOD: 3.0 pg/mL ( $S/N = 3$ ); Real sample analysis: accuracy of ProGRP determination in 11 serum samples; High selectivity, reproducibility and stability	[52]
Multi-wall carbon nanotubes	Organic electrochemical transistor (OECTs)	Sialic acid	Linear range: 0.1 to 7 mM ( $R^2 = 0.999$ ); Excellent specificity; Excellent performance for detection sialic acid in serum samples from lung cancer patients	[97]
Reduced-graphene oxide	DPV	Cytokeratin 19 fragment 21-1	Linear range: $1.0 \times 10^{-14}$ ~ $1.0 \times 10^{-6}$ M, ( $R^2 = 0.996$ and $R^2 = 0.9955$ ); LOD: 2.4 fM; Good selectivity and reproducibility	[24]
Carbon nanotubes	DPV	Lung cancer biomarkers (anti-MAGE A2 and anti-MAGE A11)	Linear range: $5 \text{ fg mL}^{-1}$ ~ $50 \text{ ng mL}^{-1}$ , ( $R^2 = 0.9939$ for anti-MAGE A2 and $R^2 = 0.9879$ for anti-MAGE A11); Detecting anti-MAGE A2 and anti-MAGE A11 simultaneously; Decreasing the time of experimental assessment and cost	[51]

### 3.6. Electrochemical Biosensors for Other Human Respiratory Diseases Diagnosis

In addition to the above electrochemical biosensors based on carbon nanomaterials for diagnosis of influenza, COVID-19, pulmonary fibrosis, tuberculosis and lung cancer, there are other reports about electrochemical biosensors based on carbon nanomaterials for diagnosis of other human respiratory diseases such as allergic rhinitis, Middle East respiratory syndrome (MERS), deep vein thrombosis, asthma and pneumonia [98–101]. These electrochemical biosensors have been fabricated by using carbon nanomaterials such

as graphene oxide, reduced graphene oxide and carbon nanotubes for detection biomarkers/microorganism of human respiratory diseases; the biomarkers include tryptase, MERS nanovesicle, D-dimer and pathogenic microorganisms. Additionally, these electrochemical biosensors also have excellent performance; details are shown in Table 6.

**Table 6.** Other electrochemical biosensors based on carbon nanomaterials for human respiratory diseases diagnosis.

Human Respiratory Diseases	Carbon Nanomaterials	Mechanism of Detection	Target	Analytical Performances	Ref.
Allergic rhinitis	Reduced graphene oxide nanocomposites	SWV	tryptase	Linear range: 100 pg/mL~100 ng/mL, ( $R^2 = 0.998$ ); LOD: 50 pg/mL ( $S/N = 3$ ); A sensitivity of 1.64 $\mu\text{A}/(\text{ng}/\text{mL})$ ; High selectivity, reproducibility (RSD 2.1%) and high stability over 1 month	[98]
Middle East respiratory syndrome (MERS)	Graphene oxide	EIS and Surface enhanced Raman spectroscopy (SERS)	MERS nanovesicle	Linear range: 1 pg/mL~100 ng/mL, ( $R^2 = 0.992$ for SERS, $R^2 = 0.9905$ for EIS); In PBS buffer, LOD: 0.176 pg/mL for SERS, LOD: 0.405 pg/mL for EIS; In diluted 10% saliva, LOD: 0.52 pg/mL for SERS, LOD: 0.645 pg/mL for EIS	[99]
Deep vein thrombosis	Functionalized carbon nanotubes	EIS	D-dimer	Linear range: 0.1 pg/mL~2 $\mu\text{g}/\text{mL}$ ; LOD: 0.1 pg/mL; Good sensitivity ( $40.1 \text{ k}\Omega\mu\text{M}^{-1}$ ); Short response time (10 min); Good reproducibility (RSD 8.2%, $n = 4$ )	[100]
Asthma/pneumonia	Single walled carbon nanotubes	EIS	Pathogenic microorganism	Linear range: $10^2$ ~ $10^{10}$ CFU/mL; LOD: $10^2$ CFU/mL; Speed response time (about 10 min); High specificity	[101]

#### 4. Comparative Analysis with Conventional Approaches for the Diagnosis of Human Respiratory Diseases

In this review, we summarize electrochemical biosensors based on carbon nanomaterials for diagnosis of human respiratory diseases. Compared with other biosensors for diagnosis of human respiratory diseases, the biosensors summarized in this review not only show the advantages of carbon nanomaterials, such as stable properties and easy preparation, but also show the advantages of electrochemical strategies such as low detection limit and fast reaction time. Taking COVID-19 as an example, Table 7 shows details of comparisons of different biosensors for diagnosis of human respiratory diseases with electrochemical biosensors based on carbon nanomaterials.

**Table 7.** Comparisons and characteristics of different biosensors for human respiratory diseases diagnosis (taking COVID-19 as an example).

Type of Biosensing Platform	Core Materials	Target	Characteristics/Remarks	Ref.
Electrochemical biosensor	Carbon nanomaterials (carbon nanotubes)	SARS-CoV-2 S1 antigen	Linear range: 0.1~5000 fg/mL; LOD: 4.12 fg/mL; Good selectivity to SARS-CoV-2 S1, Able to discriminate SARS-CoV-2 S1, SARS-CoV-1 S1 and MERS-CoV S1 antigens; Rapidly testing people for SARS-CoV2 infection; Easy to handle	[79]
Electrochemical biosensor	gold nanoparticles and coated with graphene	SARS-CoV-2 S1 antigen	Quantitatively detection at a concentration as low as picomole within 10~12 s in human plasma samples	[102]

Table 7. Cont.

Type of Biosensing Platform	Core Materials	Target	Characteristics/Remarks	Ref.
Biosensor based on frequency magnetic mixing technology	Superparamagnetic nanoparticles	SARS-CoV-2 S1 antigen	Giving qualitative and semiquantitative results of SARS-CoV-2-specific antibody levels in patient's sera within 21 min of assay time with a sensitivity of 97% and a specificity of 92%	[103]
Biosensor based on field-effect transistor	In <sub>2</sub> O <sub>3</sub> nanoribbon transistors	SARS-CoV-2 S1 antigen	detection of SARS-CoV-2 spike protein in both phosphate-buffered saline (PBS) buffer and universal transport medium (LOD: 100 fg/mL)	[104]
Biosensor based on organic field effect transistor	Semiconducting polymer	SARS-CoV-2 S1 antigen	a sensitivity of 32%/dec and a LOD of 76.61 pg/mL for SARS-CoV-2 antigen detection	[105]
Biosensor based on surface plasmon resonance	Polydopamine Ag nanoparticle	SARS-CoV-2 S1 antigen	Wide linear range of 0.0001 to 1000 ng/mL with a LOD of 12 fg/mL (S/N = 3)	[106]

## 5. Conclusions and Outlooks

In summary, this article provides a concise overview of recent studies on electrochemical biosensors based on carbon nanomaterials for the diagnosis of several important human respiratory diseases, including influenza, COVID-19, pulmonary fibrosis, tuberculosis and lung cancer. We firstly summarize the electrochemical application of carbon nanomaterials for diagnosis of various respiratory diseases in one review. Compared with other reviews related to human respiratory diseases, this review provides a comprehensive analysis of the unique characteristics of carbon nanomaterials and the advantages of electrochemical assays for diagnosis of human respiratory diseases. Besides, compared with other traditional methods for diagnosis of human respiratory diseases, these electrochemical biosensors based on carbon nanomaterials which are summarized in this review are simple, fast-operating diagnostic procedures for diagnosis of respiratory diseases in the early stage by detection of respiratory viruses, related DNA fragments, proteins or RNA. In addition, these biosensors have shown great potential for both basic research and clinical applications in the field of alerting and preventing the spread of respiratory diseases.

There are, however, still many significant challenges that need to be overcome before the research and development of these biosensors successfully translate into clinical practices. The challenges include, but are not limited to (1) the fact that the current electrochemical biosensors based on carbon nanomaterials can detect only a limited number of respiratory viruses, related DNA fragments, proteins and RNAs, (2) carbon nanomaterials as electrode materials in some electrochemical biosensors for the diagnosis of respiratory diseases only play a small role and their excellent properties have not been fully utilized, which is far from the materials' full potential, and (3) the current range of electrochemical biosensors based on carbon nanomaterials have some restrictions, such as restrictions in terms of the limit of detection and range of linearity, in the diagnosis of respiratory diseases.

Thus, in future research and development of electrochemical biosensors based on carbon nanomaterials for diagnosis of respiratory diseases, efforts should be made to exploit not only more biomarkers related to respiratory diseases, but also more functions of the carbon nanomaterials so to develop them into mainstream materials for fabrication of electrochemical biosensors. Further, the detection limit and range of linearity of the electrochemical biosensor based on carbon nanomaterials for diagnosis of respiratory diseases should be optimized. In addition, new synthetic methods of carbon nanomaterials should be exploited to make them possess better optical, electrical and other properties. Finally, due to the excellent application potential of carbon nanomaterials in electrochemical

biosensors for diagnosis of human respiratory diseases, carbon nanomaterials should be exploited to be the main electrode materials.

**Author Contributions:** Conceptualization, C.L. and L.D.; writing—original draft preparation, C.L., B.C. and L.D.; writing—review and editing, C.L. and L.D.; supervision, C.L. and L.D.; project administration, C.L. and L.D.; funding acquisition, L.D. All authors have read and agreed to the published version of the manuscript.

**Funding:** This work was partially supported financially by grants of the Natural Science Foundation of China (Grants No. 12272063, 11532003, 31670950).

**Institutional Review Board Statement:** Not applicable.

**Informed Consent Statement:** Not applicable.

**Data Availability Statement:** Not applicable.

**Conflicts of Interest:** The authors declare no conflict of interest.

## References

1. Khattak, S.; Zhang, Q.-Q.; Sarfraz, M.; Muhammad, P.; Ngowi, E.E.; Khan, N.H.; Rauf, S.; Wang, Y.-Z.; Qi, H.-W.; Wang, D.; et al. The Role of Hydrogen Sulfide in Respiratory Diseases. *Biomolecules* **2021**, *11*, 682. [[CrossRef](#)] [[PubMed](#)]
2. Chan, Y.; Ng, S.W.; Singh, S.K.; Gulati, M.; Gupta, G.; Chaudhary, S.K.; Hing, G.B.; Collet, T.; MacLoughlin, R.; Lobenberg, R.; et al. Revolutionizing polymer-based nanoparticle-linked vaccines for targeting respiratory viruses: A perspective. *Life Sci.* **2021**, *280*, 119744. [[CrossRef](#)] [[PubMed](#)]
3. De Jong, P.A.; Nakano, Y.; Lequin, M.H.; Mayo, J.R.; Woods, R.; Pare, P.D.; Tiddens, H.A. Progressive damage on high resolution computed tomography despite stable lung function in cystic fibrosis. *Eur. Respir. J.* **2004**, *23*, 93–97. [[CrossRef](#)] [[PubMed](#)]
4. Ong, D.S.; Fragkou, P.C.; Schweitzer, V.A.; Chemaly, R.F.; Moschopoulos, C.D.; Skevaki, C. How to interpret and use COVID-19 serology and immunology tests. *Clin. Microbiol. Infect.* **2021**, *27*, 981–986. [[CrossRef](#)] [[PubMed](#)]
5. Niel, C.; Ricordel, C.; Guy, T.; Kerjouan, M.; De Latour, B.; Chiforeanu, D.; Lederlin, M.; Jouneau, S. Idiopathic pulmonary fibrosis diagnosed concomitantly with diffuse squamous cell lung cancer on surgical lung biopsy: A case report. *J. Med. Case Rep.* **2021**, *15*, 595. [[CrossRef](#)]
6. Zhu, X.; Ai, S.; Chen, Q.; Yin, H.; Xu, J. Label-free electrochemical detection of Avian Influenza Virus genotype utilizing multi-walled carbon nanotubes-cobalt phthalocyanine-PAMAM nanocomposite modified glassy carbon electrode. *Electrochem. Commun.* **2009**, *11*, 1543–1546. [[CrossRef](#)]
7. Mahshid, S.S.; Flynn, S.E.; Mahshid, S. The potential application of electrochemical biosensors in the COVID-19 pandemic: A perspective on the rapid diagnostics of SARS-CoV-2. *Biosens. Bioelectron.* **2021**, *176*, 112905. [[CrossRef](#)]
8. Abid, S.A.; Ahmed Muneer, A.; Al-Kadmy, I.M.S.; Sattar, A.A.; Beshbishy, A.M.; Batiha, G.E.; Hetta, H.F. Biosensors as a future diagnostic approach for COVID-19. *Life Sci.* **2021**, *273*, 119117. [[CrossRef](#)]
9. Khanmohammadi, A.; Aghaie, A.; Vahedi, E.; Qazvini, A.; Ghanei, M.; Afkhami, A.; Hajian, A.; Bagheri, H. Electrochemical biosensors for the detection of lung cancer biomarkers: A review. *Talanta* **2020**, *206*, 120251. [[CrossRef](#)]
10. Tepeli, Y.; Ülkü, A. Electrochemical biosensors for influenza virus a detection: The potential of adaptation of these devices to POC systems. *Sens. Actuators B Chem.* **2018**, *254*, 377–384. [[CrossRef](#)]
11. Pang, S.-N.; Lin, Y.-L.; Yu, K.-J.; Chiou, Y.-E.; Leung, W.-H.; Weng, W.-H. An Effective SARS-CoV-2 Electrochemical Biosensor with Modifiable Dual Probes Using a Modified Screen-Printed Carbon Electrode. *Micromachines* **2021**, *12*, 1171. [[CrossRef](#)]
12. Kaya, H.O.; Cetin, A.E.; Azimzadeh, M.; Topkaya, S.N. Pathogen detection with electrochemical biosensors: Advantages, challenges and future perspectives. *J. Electroanal. Chem.* **2021**, *882*, 114989. [[CrossRef](#)]
13. Long, D.; Li, M.; Wang, H.; Wang, H.; Chai, Y.; Yuan, R. A photoelectrochemical biosensor based on fullerene with methylene blue as a sensitizer for ultrasensitive DNA detection. *Biosens. Bioelectron.* **2019**, *142*, 111579. [[CrossRef](#)]
14. Khan, M.Z.H.; Hasan, M.R.; Hossain, S.I.; Ahommed, M.S.; Daizy, M. Ultrasensitive detection of pathogenic viruses with electrochemical biosensor: State of the art. *Biosens. Bioelectron.* **2020**, *166*, 112431. [[CrossRef](#)]
15. Golichenari, B.; Nosrati, R.; Farokhi-Fard, A.; Faal Maleki, M.; Gheibi Hayat, S.M.; Ghazvini, K.; Vaziri, F.; Behravan, J. Electrochemical-based biosensors for detection of Mycobacterium tuberculosis and tuberculosis biomarkers. *Crit. Rev. Biotechnol.* **2019**, *39*, 1056–1077. [[CrossRef](#)]
16. Mogha, N.K.; Sahu, V.; Sharma, R.K.; Masram, D.T. Reduced graphene oxide nanoribbon immobilized gold nanoparticle based electrochemical DNA biosensor for the detection of Mycobacterium tuberculosis. *J. Mater. Chem. B* **2018**, *6*, 5181–5187. [[CrossRef](#)]
17. Liu, C.; Jiang, D.; Xiang, G.; Liu, L.; Liu, F.; Pu, X. An electrochemical DNA biosensor for the detection of Mycobacterium tuberculosis, based on signal amplification of graphene and a gold nanoparticle-polyaniline nanocomposite. *Analyst* **2014**, *139*, 5460–5465. [[CrossRef](#)]

18. Chen, Y.; Guo, S.; Zhao, M.; Zhang, P.; Xin, Z.; Tao, J.; Bai, L. Amperometric DNA biosensor for Mycobacterium tuberculosis detection using flower-like carbon nanotubes-polyaniline nanohybrid and enzyme-assisted signal amplification strategy. *Biosens. Bioelectron.* **2018**, *119*, 215–220. [[CrossRef](#)]
19. Bai, L.; Chen, Y.; Liu, X.; Zhou, J.; Cao, J.; Hou, L.; Guo, S. Ultrasensitive electrochemical detection of Mycobacterium tuberculosis IS6110 fragment using gold nanoparticles decorated fullerene nanoparticles/nitrogen-doped graphene nanosheet as signal tags. *Anal. Chim. Acta* **2019**, *1080*, 75–83. [[CrossRef](#)]
20. Zuo, J.; Yuan, Y.; Zhao, M.; Wang, J.; Chen, Y.; Zhu, Q.; Bai, L. An efficient electrochemical assay for miR-3675-3p in human serum based on the nanohybrid of functionalized fullerene and metal-organic framework. *Anal. Chim. Acta* **2020**, *1140*, 78–88. [[CrossRef](#)]
21. Amouzadeh Tabrizi, M.; Shamsipur, M.; Farzin, L. A high sensitive electrochemical aptasensor for the determination of VEGF(165) in serum of lung cancer patient. *Biosens. Bioelectron.* **2015**, *74*, 764–769. [[CrossRef](#)] [[PubMed](#)]
22. Zhang, Q.; Li, X.; Qian, C.; Dou, L.; Cui, F.; Chen, X. Label-free electrochemical immunoassay for neuron specific enolase based on 3D macroporous reduced graphene oxide/polyaniline film. *Anal. Biochem.* **2018**, *540–541*, 1–8. [[CrossRef](#)] [[PubMed](#)]
23. Deepa; Nohwal, B.; Pundir, C.S. An electrochemical CD59 targeted noninvasive immunosensor based on graphene oxide nanoparticles embodied pencil graphite for detection of lung cancer. *Microchem. J.* **2020**, *156*, 104957. [[CrossRef](#)]
24. Jafari-Kashi, A.; Rafiee-Pour, H.A.; Shabani-Nooshabadi, M. A new strategy to design label-free electrochemical biosensor for ultrasensitive diagnosis of CYFRA 21-1 as a biomarker for detection of non-small cell lung cancer. *Chemosphere* **2022**, *301*, 134636. [[CrossRef](#)] [[PubMed](#)]
25. Li, C.; Wang, Y.; Jiang, H.; Wang, X. Review-Intracellular sensors based on carbonaceous nanomaterials: A review. *J. Electrochem. Soc.* **2020**, *167*, 037540. [[CrossRef](#)]
26. Xie, P.; Yuan, W.; Liu, X.; Peng, Y.; Yin, Y.; Li, Y.; Wu, Z. Advanced carbon nanomaterials for state-of-the-art flexible supercapacitors. *Energy Storage Mater.* **2021**, *36*, 56–76. [[CrossRef](#)]
27. Karimi-Maleh, H.; Beitollahi, H.; Senthil Kumar, P.; Tajik, S.; Mohammadzadeh Jahani, P.; Karimi, F.; Karaman, C.; Vasseghian, Y.; Baghayeri, M.; Rouhi, J.; et al. Recent advances in carbon nanomaterials-based electrochemical sensors for food azo dyes detection. *Food Chem. Toxicol.* **2022**, *164*, 112961. [[CrossRef](#)]
28. Chen, M.; Wu, D.; Tu, S.; Yang, C.; Chen, D.; Xu, Y. A novel biosensor for the ultrasensitive detection of the lncRNA biomarker MALAT1 in non-small cell lung cancer. *Sci. Rep.* **2021**, *11*, 3666. [[CrossRef](#)]
29. Gutierrez-Galvez, L.; Del Cano, R.; Menendez-Luque, I.; Garcia-Nieto, D.; Rodriguez-Pena, M.; Luna, M.; Pineda, T.; Pariente, F.; Garcia-Mendiola, T.; Lorenzo, E. Electrochemiluminescent nanostructured DNA biosensor for SARS-CoV-2 detection. *Talanta* **2022**, *240*, 123203. [[CrossRef](#)]
30. Saadati, A.; Hassanpour, S.; Hasanzadeh, M.; Shadjou, N. Binding of pDNA with cDNA using hybridization strategy towards monitoring of Haemophilus influenza genome in human plasma samples. *Int. J. Biol. Macromol.* **2020**, *150*, 218–227. [[CrossRef](#)]
31. Miller, L.A.; Royer, C.M.; Pinkerton, K.E.; Schelegle, E.S. Nonhuman primate models of respiratory disease: Past, present, and future. *ILAR J.* **2017**, *58*, 269–280. [[CrossRef](#)]
32. Szalontai, K.; Gemes, N.; Furak, J.; Varga, T.; Neuperger, P.; Balog, J.A.; Puskas, L.G.; Szebeni, G.J. Chronic obstructive pulmonary disease: Epidemiology, biomarkers, and paving the way to lung cancer. *J. Clin. Med.* **2021**, *10*, 2889. [[CrossRef](#)]
33. Aminian, A.R.; Mohebbati, R.; Boskabady, M.H. The effect of *Ocimum basilicum* L. and its main ingredients on respiratory disorders: An experimental, preclinical, and clinical review. *Front. Pharmacol.* **2021**, *12*, 805391. [[CrossRef](#)]
34. Alharbi, K.S.; Fuloria, N.K.; Fuloria, S.; Rahman, S.B.; Al-Malki, W.H.; Javed Shaikh, M.A.; Thangavelu, L.; Singh, S.K.; Rama Raju Allam, V.S.; Jha, N.K.; et al. Nuclear factor-kappa B and its role in inflammatory lung disease. *Chem. Biol. Interact.* **2021**, *345*, 109568. [[CrossRef](#)]
35. Nidzworski, D.; Siuzdak, K.; Niedzialkowski, P.; Bogdanowicz, R.; Sobaszek, M.; Ryl, J.; Weiher, P.; Sawczak, M.; Wnuk, E.; Goddard, W.A., 3rd; et al. A rapid-response ultrasensitive biosensor for influenza virus detection using antibody modified boron-doped diamond. *Sci. Rep.* **2017**, *7*, 15707. [[CrossRef](#)]
36. Yang, J.; Xiang, Y.; Song, C.; Liu, L.; Jing, X.; Xie, G.; Xiang, H. Quadruple signal amplification strategy based on hybridization chain reaction and an immunoelectrode modified with graphene sheets, a hemin/G-quadruplex DNAzyme concatamer, and alcohol dehydrogenase: Ultrasensitive determination of influenza virus subtype H7N9. *Microchim. Acta* **2015**, *182*, 2377–2385. [[CrossRef](#)]
37. Liu, X.; Cheng, Z.; Fan, H.; Ai, S.; Han, R. Electrochemical detection of avian influenza virus H5N1 gene sequence using a DNA aptamer immobilized onto a hybrid nanomaterial-modified electrode. *Electrochim. Acta* **2011**, *56*, 6266–6270. [[CrossRef](#)]
38. Lee, D.; Chander, Y.; Goyal, S.M.; Cui, T. Carbon nanotube electric immunoassay for the detection of swine influenza virus H1N1. *Biosens. Bioelectron.* **2011**, *26*, 3482–3487. [[CrossRef](#)]
39. Kinnamon, D.S.; Krishnan, S.; Brosler, S.; Sun, E.; Prasad, S. Screen printed graphene oxide textile biosensor for applications in inexpensive and wearable point-of-exposure detection of influenza for at-risk populations. *J. Electrochem. Soc.* **2018**, *165*, B3084–B3090. [[CrossRef](#)]
40. Jain, R.; Nirbhaya, V.; Chandra, R.; Kumar, S. Nanostructured mesoporous carbon based electrochemical biosensor for efficient detection of swine flu. *Electroanalysis* **2021**, *34*, 43–55. [[CrossRef](#)]
41. Devarakonda, S.; Singh, R.; Bhardwaj, J.; Jang, J. Cost-effective and handmade paper-based immunosensing device for electrochemical detection of influenza virus. *Sensors* **2017**, *17*, 2597. [[CrossRef](#)] [[PubMed](#)]
42. Palmieri, V.; Papi, M. Can graphene take part in the fight against COVID-19? *Nano Today* **2020**, *33*, 100883. [[CrossRef](#)] [[PubMed](#)]

43. Shang, Z.; Chan, S.Y.; Liu, W.J.; Li, P.; Huang, W. Recent insights into emerging coronavirus: SARS-CoV-2. *ACS Infect. Dis.* **2021**, *7*, 1369–1388. [[CrossRef](#)] [[PubMed](#)]
44. Seo, G.; Lee, G.; Kim, M.J.; Baek, S.H.; Choi, M.; Ku, K.B.; Lee, C.S.; Jun, S.; Park, D.; Kim, H.G.; et al. Rapid detection of COVID-19 causative virus (SARS-CoV-2) in human nasopharyngeal swab specimens using field-effect transistor-based biosensor. *ACS Nano* **2020**, *14*, 5135–5142. [[CrossRef](#)] [[PubMed](#)]
45. Srivastava, M.; Srivastava, N.; Mishra, P.K.; Malhotra, B.D. Prospects of nanomaterials-enabled biosensors for COVID-19 detection. *Sci. Total Environ.* **2021**, *754*, 142363. [[CrossRef](#)]
46. Beduk, T.; Beduk, D.; de Oliveira Filho, J.I.; Zihnioglu, F.; Cicek, C.; Serto, R.; Arda, B.; Goksel, T.; Turhan, K.; Salama, K.N.; et al. Rapid point-of-care COVID-19 diagnosis with a gold-nanoarchitecture-assisted laser-scribed graphene biosensor. *Anal. Chem.* **2021**, *93*, 8585–8594. [[CrossRef](#)]
47. Ang, W.L.; Lim, R.R.X.; Ambrosi, A.; Bonanni, A. Rapid electrochemical detection of COVID-19 genomic sequence with dual-function graphene nanocolloids based biosensor. *FlatChem* **2022**, *32*, 100336. [[CrossRef](#)]
48. Bonanni, A.; Pividori, M.I.; del Valle, M. DNA polymorphism sensitive impedimetric detection on gold-nanoislands modified electrodes. *Talanta* **2015**, *136*, 95–101. [[CrossRef](#)]
49. Pai, M.; Behr, M.A.; Dowdy, D.; Dheda, K.; Divangahi, M.; Boehme, C.C.; Ginsberg, A.; Swaminathan, S.; Spigelman, M.; Getahun, H.; et al. Tuberculosis. *Nat. Rev. Dis. Prim.* **2016**, *2*, 16076. [[CrossRef](#)]
50. Thai, A.A.; Solomon, B.J.; Sequist, L.V.; Gainor, J.F.; Heist, R.S. Lung cancer. *Lancet* **2021**, *398*, 535–554. [[CrossRef](#)]
51. Choudhary, M.; Singh, A.; Kaur, S.; Arora, K. Enhancing lung cancer diagnosis: Electrochemical simultaneous bioanalyte immunosensing using carbon nanotubes-chitosan nanocomposite. *Appl. Biochem. Biotechnol.* **2014**, *174*, 1188–1200. [[CrossRef](#)]
52. Zhuo, Y.; Chai, Y.Q.; Yuan, R.; Mao, L.; Yuan, Y.L.; Han, J. Glucose oxidase and ferrocene labels immobilized at Au/TiO<sub>2</sub> nanocomposites with high load amount and activity for sensitive immunoelectrochemical measurement of ProGRP biomarker. *Biosens. Bioelectron.* **2011**, *26*, 3838–3844. [[CrossRef](#)]
53. Cui, T.-R.; Qiao, Y.-C.; Gao, J.-W.; Wang, C.-H.; Zhang, Y.; Han, L.; Yang, Y.; Ren, T.-L. Ultrasensitive Detection of COVID-19 Causative Virus (SARS-CoV-2) Spike Protein Using Laser Induced Graphene Field-Effect Transistor. *Molecules* **2021**, *26*, 6947. [[CrossRef](#)]
54. Touw, H.R.; Parlevliet, K.L.; Beerepoot, M.; Schober, P.; Vonk, A.; Twisk, J.W.; Elbers, P.W.; Boer, C.; Tuinman, P.R. Lung ultrasound compared with chest X-ray in diagnosing postoperative pulmonary complications following cardiothoracic surgery: A prospective observational study. *Anaesthesia* **2018**, *73*, 946–954. [[CrossRef](#)]
55. Choudhury, P.; Biswas, S.; Singh, G.; Pal, A.; Ghosh, N.; Ojha, A.K.; Das, S.; Dutta, G.; Chaudhury, K. Immunological profiling and development of a sensing device for detection of IL-13 in COPD and asthma. *Bioelectrochemistry* **2022**, *143*, 107971. [[CrossRef](#)]
56. Fang, L.-X.; Cao, J.-T.; Huang, K.-J. A sensitive electrochemical biosensor for specific DNA sequence detection based on flower-like VS<sub>2</sub>, graphene and Au nanoparticles signal amplification. *J. Electroanal. Chem.* **2015**, *746*, 1–8. [[CrossRef](#)]
57. Zheng, X.T.; Ananthanarayanan, A.; Luo, K.Q.; Chen, P. Glowing graphene quantum dots and carbon dots: Properties, syntheses, and biological applications. *Small* **2015**, *11*, 1620–1636. [[CrossRef](#)]
58. Feng, H.; Qian, Z. Functional carbon quantum dots: A versatile platform for chemosensing and biosensing. *Chem. Rec.* **2018**, *18*, 491–505. [[CrossRef](#)]
59. Pumera, M. Electrochemistry of graphene, graphene oxide and other graphenoids: Review. *Electrochem. Commun.* **2013**, *36*, 14–18. [[CrossRef](#)]
60. Idris, A.O.; Oseghe, E.O.; Msagati, T.A.M.; Kuvarega, A.T.; Feloni, U.; Mamba, B. Graphitic Carbon Nitride: A Highly Electroactive Nanomaterial for Environmental and Clinical Sensing. *Sensors* **2020**, *20*, 5743. [[CrossRef](#)]
61. Yao, S.; Yuan, X.; Jiang, L.; Xiong, T.; Zhang, J. Recent Progress on Fullerene-Based Materials: Synthesis, Properties, Modifications, and Photocatalytic Applications. *Materials* **2020**, *13*, 2924. [[CrossRef](#)] [[PubMed](#)]
62. Ramanathan, S.; Gopinath, S.C.B.; Ismail, Z.H.; Md Arshad, M.K.; Poopalan, P. Aptasensing nucleocapsid protein on nanodiamond assembled gold interdigitated electrodes for impedimetric SARS-CoV-2 infectious disease assessment. *Biosens. Bioelectron.* **2022**, *197*, 113735. [[CrossRef](#)] [[PubMed](#)]
63. Jian, Z.; Xu, J.; Yang, N.; Han, S.; Jiang, X. A perspective on diamond composites and their electrochemical applications. *Curr. Opin. Electrochem.* **2021**, *30*, 100835. [[CrossRef](#)]
64. Zhao, H.; Liu, F.; Xie, W.; Zhou, T.C.; OuYang, J.; Jin, L.; Li, H.; Zhao, C.Y.; Zhang, L.; Wei, J.; et al. Ultrasensitive supersandwich-type electrochemical sensor for SARS-CoV-2 from the infected COVID-19 patients using a smartphone. *Sens. Actuators B Chem.* **2021**, *327*, 128899. [[CrossRef](#)] [[PubMed](#)]
65. Yang, H.; Bao, J.; Huo, D.; Zeng, Y.; Wang, X.; Samalo, M.; Zhao, J.; Zhang, S.; Shen, C.; Hou, C. Au doped poly-thionine and poly-m-Cresol purple: Synthesis and their application in simultaneously electrochemical detection of two lung cancer markers CEA and CYFRA21-1. *Talanta* **2021**, *224*, 121816. [[CrossRef](#)]
66. Bhardwaj, J.; Kim, M.W.; Jang, J. Rapid airborne influenza virus quantification using an antibody-based electrochemical paper sensor and electrostatic particle concentrator. *Environ. Sci. Technol.* **2020**, *54*, 10700–10712. [[CrossRef](#)]
67. Xu, L.; Jiang, X.; Zhu, Y.; Duan, Y.; Huang, T.; Huang, Z.; Liu, C.; Xu, B.; Xie, Z. A multiplex asymmetric reverse transcription-PCR assay combined with an electrochemical DNA sensor for simultaneously detecting and subtyping influenza A viruses. *Front. Microbiol.* **2018**, *9*, 1405. [[CrossRef](#)]

68. Siuzdak, K.; Niedziałkowski, P.; Sobaszek, M.; Łęga, T.; Sawczak, M.; Czaczyk, E.; Dziąbowska, K.; Ossowski, T.; Nidzworski, D.; Bogdanowicz, R. Biomolecular influenza virus detection based on the electrochemical impedance spectroscopy using the nanocrystalline boron-doped diamond electrodes with covalently bound antibodies. *Sens. Actuators B Chem.* **2019**, *280*, 263–271. [[CrossRef](#)]
69. Lee, D.; Bhardwaj, J.; Jang, J. Paper-based electrochemical immunosensor for label-free detection of multiple avian influenza virus antigens using flexible screen-printed carbon nanotube-polydimethylsiloxane electrodes. *Sci. Rep.* **2022**, *12*, 2311. [[CrossRef](#)]
70. Manohara Reddy, Y.V.; Shin, J.H.; Hwang, J.; Kweon, D.H.; Choi, C.H.; Park, K.; Kim, S.K.; Madhavi, G.; Yi, H.; Park, J.P. Fine-tuning of MXene-nickel oxide-reduced graphene oxide nanocomposite bioelectrode: Sensor for the detection of influenza virus and viral protein. *Biosens. Bioelectron.* **2022**, *214*, 114511. [[CrossRef](#)]
71. Anik, U.; Tepeli, Y.; Sayhi, M.; Nsiri, J.; Diouani, M.F. Towards the electrochemical diagnostic of influenza virus: Development of a graphene-Au hybrid nanocomposite modified influenza virus biosensor based on neuraminidase activity. *Analyst* **2017**, *143*, 150–156. [[CrossRef](#)]
72. Lamers, M.M.; Haagmans, B.L. SARS-CoV-2 pathogenesis. *Nat. Rev. Microbiol.* **2022**, *20*, 270–284. [[CrossRef](#)]
73. Wang, C.C.; Prather, K.A.; Sznitman, J.; Jimenez, J.L.; Lakdawala, S.S.; Tufekci, Z.; Marr, L.C. Airborne transmission of respiratory viruses. *Science* **2021**, *373*, eabd9149. [[CrossRef](#)]
74. Synowiec, A.; Szczepanski, A.; Barreto-Duran, E.; Lie, L.K.; Pyrc, K. Severe acute respiratory syndrome coronavirus 2 (SARS-CoV-2): A systemic infection. *Clin. Microbiol. Rev.* **2021**, *34*, e00133-20. [[CrossRef](#)]
75. Fahmy, H.M.; Abu Serea, E.S.; Salah-Eldin, R.E.; Al-Hafiry, S.A.; Ali, M.K.; Shalan, A.E.; Lanceros-Mendez, S. Recent progress in graphene- and related carbon-nanomaterial-based electrochemical biosensors for early disease detection. *ACS Biomater. Sci. Eng.* **2022**, *8*, 964–1000. [[CrossRef](#)]
76. Liv, L.; Coban, G.; Nakiboglu, N.; Kocagoz, T. A rapid, ultrasensitive voltammetric biosensor for determining SARS-CoV-2 spike protein in real samples. *Biosens. Bioelectron.* **2021**, *192*, 113497. [[CrossRef](#)]
77. Bialobrzeska, W.; Ficek, M.; Dec, B.; Osella, S.; Trzaskowski, B.; Jaramillo-Botero, A.; Pierpaoli, M.; Ryciewicz, M.; Dashkevich, Y.; Lega, T.; et al. Performance of electrochemical immunoassays for clinical diagnostics of SARS-CoV-2 based on selective nucleocapsid N protein detection: Boron-doped diamond, gold and glassy carbon evaluation. *Biosens. Bioelectron.* **2022**, *209*, 114222. [[CrossRef](#)]
78. Stefano, J.S.; Guterres, E.S.L.R.; Rocha, R.G.; Brazaca, L.C.; Richter, E.M.; Abarza Munoz, R.A.; Janegitz, B.C. New conductive filament ready-to-use for 3D-printing electrochemical (bio)sensors: Towards the detection of SARS-CoV-2. *Anal. Chim. Acta* **2022**, *1191*, 339372. [[CrossRef](#)]
79. Zamzami, M.A.; Rabhani, G.; Ahmad, A.; Basalah, A.A.; Al-Sabban, W.H.; Nate Ahn, S.; Choudhry, H. Carbon nanotube field-effect transistor (CNT-FET)-based biosensor for rapid detection of SARS-CoV-2 (COVID-19) surface spike protein S1. *Bioelectrochemistry* **2022**, *143*, 107982. [[CrossRef](#)]
80. García-Mendiola, T.; Bravo, I.; López-Moreno, J.M.; Pariente, F.; Wannemacher, R.; Weber, K.; Popp, J.; Lorenzo, E. Carbon nanodots based biosensors for gene mutation detection. *Sens. Actuators B Chem.* **2018**, *256*, 226–233. [[CrossRef](#)]
81. Eissa, S.; Alshehri, N.; Abduljabbar, M.; Rahman, A.M.A.; Dasouki, M.; Nizami, I.Y.; Al-Muhaizea, M.A.; Zourob, M. Carbon nanofiber-based multiplexed immunosensor for the detection of survival motor neuron 1, cystic fibrosis transmembrane conductance regulator and Duchenne Muscular Dystrophy proteins. *Biosens. Bioelectron.* **2018**, *117*, 84–90. [[CrossRef](#)] [[PubMed](#)]
82. Mahomed, S.; Mlisana, K.; Cele, L.; Naidoo, K. Discordant line probe genotypic testing vs culture-based drug susceptibility phenotypic testing in TB endemic KwaZulu-Natal: Impact on bedside clinical decision making. *J. Clin. Tuberc. Other Mycobact. Dis.* **2020**, *20*, 100176. [[CrossRef](#)] [[PubMed](#)]
83. Thakur, H.; Kaur, N.; Sabherwal, P.; Sareen, D.; Prabhakar, N. Aptamer based voltammetric biosensor for the detection of Mycobacterium tuberculosis antigen MPT64. *Microchim. Acta* **2017**, *184*, 1915–1922. [[CrossRef](#)]
84. Zaid, M.H.M.; Abdullah, J.; Yusof, N.A.; Wasoh, H.; Sulaiman, Y.; Noh, M.F.M.; Issa, R. Reduced graphene oxide/TEMPO-nanocellulose nanohybrid-based electrochemical biosensor for the determination of Mycobacterium tuberculosis. *J. Sens.* **2020**, *2020*, 4051474. [[CrossRef](#)]
85. Gou, D.; Xie, G.; Li, Y.; Zhang, X.; Chen, H. Voltammetric immunoassay for Mycobacterium tuberculosis secretory protein MPT64 based on a synergistic amplification strategy using rolling circle amplification and a gold electrode modified with graphene oxide, Fe<sub>3</sub>O<sub>4</sub> and Pt nanoparticles. *Microchim. Acta* **2018**, *185*, 436. [[CrossRef](#)]
86. Li, L.; Yuan, Y.; Chen, Y.; Zhang, P.; Bai, Y.; Bai, L. Aptamer based voltammetric biosensor for Mycobacterium tuberculosis antigen ESAT-6 using a nanohybrid material composed of reduced graphene oxide and a metal-organic framework. *Microchim. Acta* **2018**, *185*, 379. [[CrossRef](#)]
87. Chen, Y.; Li, Y.; Yang, Y.; Wu, F.; Cao, J.; Bai, L. A polyaniline-reduced graphene oxide nanocomposite as a redox nanoprobe in a voltammetric DNA biosensor for Mycobacterium tuberculosis. *Microchim. Acta* **2017**, *184*, 1801–1808. [[CrossRef](#)]
88. Mat Zaid, M.H.; Abdullah, J.; Yusof, N.A.; Sulaiman, Y.; Wasoh, H.; Md Noh, M.F.; Issa, R. PNA biosensor based on reduced graphene oxide/water soluble quantum dots for the detection of Mycobacterium tuberculosis. *Sens. Actuators B Chem.* **2017**, *241*, 1024–1034. [[CrossRef](#)]
89. Li, J.; Hu, K.; Zhang, Z.; Teng, X.; Zhang, X. Click DNA cycling in combination with gold nanoparticles loaded with quadruplex DNA motifs enable sensitive electrochemical quantitation of the tuberculosis-associated biomarker CFP-10 in sputum. *Microchim. Acta* **2019**, *186*, 662. [[CrossRef](#)]

90. Javed, A.; Abbas, S.R.; Hashmi, M.U.; Babar, N.U.A.; Hussain, I. Graphene oxide based electrochemical genosensor for label free detection of Mycobacterium tuberculosis from raw clinical samples. *Int. J. Nanomed.* **2021**, *16*, 7339–7352. [[CrossRef](#)]
91. Perumal, V.; Saheed, M.S.M.; Mohamed, N.M.; Saheed, M.S.M.; Murthe, S.S.; Gopinath, S.C.B.; Chiu, J.M. Gold nanorod embedded novel 3D graphene nanocomposite for selective bio-capture in rapid detection of Mycobacterium tuberculosis. *Biosens. Bioelectron.* **2018**, *116*, 116–122. [[CrossRef](#)]
92. Tufa, L.T.; Oh, S.; Tran, V.T.; Kim, J.; Jeong, K.-J.; Park, T.J.; Kim, H.-J.; Lee, J. Electrochemical immunosensor using nanotriplex of graphene quantum dots, Fe<sub>3</sub>O<sub>4</sub>, and Ag nanoparticles for tuberculosis. *Electrochim. Acta* **2018**, *290*, 369–377. [[CrossRef](#)]
93. Hu, J.; Zhang, Y.; Chai, Y.; Yuan, R. A novel self-enhancement NCNDs-BPEI-Ru nanocomposite with highly efficient electrochemiluminescence as signal probe for ultrasensitive detection of MTB. *Sens. Actuators B Chem.* **2022**, *354*, 131252. [[CrossRef](#)]
94. Azmi, U.Z.M.; Yusof, N.A.; Abdullah, J.; Mohammad, F.; Ahmad, S.A.A.; Suraiya, S.; Raston, N.H.A.; Faudzi, F.N.M.; Khiste, S.K.; Al-Lohedan, H.A. Aptasensor for the detection of Mycobacterium tuberculosis in sputum utilising CFP10-ESAT6 protein as a selective biomarker. *Nanomaterials* **2021**, *11*, 2446. [[CrossRef](#)]
95. Zhu, M.; Tang, Y.; Wen, Q.; Li, J.; Yang, P. Dynamic evaluation of cell-secreted interferon gamma in response to drug stimulation via a sensitive electro-chemiluminescence immunosensor based on a glassy carbon electrode modified with graphene oxide, polyaniline nanofibers, magnetic beads, and gold nanoparticles. *Microchim. Acta* **2016**, *183*, 1739–1748. [[CrossRef](#)]
96. Bairagi, P.K.; Goyal, A.; Verma, N. Methyl nicotinate biomarker of tuberculosis voltammetrically detected on cobalt nanoparticle-dispersed reduced graphene oxide-based carbon film in blood. *Sens. Actuators B Chem.* **2019**, *297*, 126754. [[CrossRef](#)]
97. Chen, L.; Wang, N.; Wu, J.; Yan, F.; Ju, H. Organic electrochemical transistor for sensing of sialic acid in serum samples. *Anal. Chim. Acta* **2020**, *1128*, 231–237. [[CrossRef](#)]
98. Lee, J.; Lee, Y.J.; Eun, Y.G.; Lee, G.J. An ultrasensitive electrochemical detection of tryptase using 3D macroporous reduced graphene oxide nanocomposites by one-pot electrochemical synthesis. *Anal. Chim. Acta* **2019**, *1069*, 47–56. [[CrossRef](#)]
99. Kim, G.; Kim, J.; Kim, S.M.; Kato, T.; Yoon, J.; Noh, S.; Park, E.Y.; Park, C.; Lee, T.; Choi, J.W. Fabrication of MERS-nanovesicle biosensor composed of multi-functional DNA aptamer/graphene-MoS<sub>2</sub> nanocomposite based on electrochemical and surface-enhanced Raman spectroscopy. *Sens. Actuators B Chem.* **2022**, *352*, 131060. [[CrossRef](#)]
100. Bourigua, S.; Hnaïen, M.; Bessueille, F.; Lagarde, F.; Dzyadevych, S.; Maaref, A.; Bausells, J.; Errachid, A.; Jaffrezic Renault, N. Impedimetric immunosensor based on SWCNT-COOH modified gold microelectrodes for label-free detection of deep venous thrombosis biomarker. *Biosens. Bioelectron.* **2010**, *26*, 1278–1282. [[CrossRef](#)]
101. Yoo, M.S.; Shin, M.; Kim, Y.; Jang, M.; Choi, Y.E.; Park, S.J.; Choi, J.; Lee, J.; Park, C. Development of electrochemical biosensor for detection of pathogenic microorganism in Asian dust events. *Chemosphere* **2017**, *175*, 269–274. [[CrossRef](#)] [[PubMed](#)]
102. Ali, M.A.; Zhang, G.F.; Hu, C.; Yuan, B.; Jahan, S.; Kitsios, G.D.; Morris, A.; Gao, S.J.; Panat, R. Ultrarapid and ultrasensitive detection of SARS-CoV-2 antibodies in COVID-19 patients via a 3D-printed nanomaterial-based biosensing platform. *J. Med. Virol.* **2022**, *94*, 5808–5826. [[CrossRef](#)] [[PubMed](#)]
103. Pietschmann, J.; Voepel, N.; Voss, L.; Rasche, S.; Schubert, M.; Kleines, M.; Krause, H.J.; Shaw, T.M.; Spiegel, H.; Schroeper, F. Development of fast and portable frequency magnetic mixing-based serological SARS-CoV-2-specific antibody detection assay. *Front. Microbiol.* **2021**, *12*, 643275. [[CrossRef](#)] [[PubMed](#)]
104. Chen, M.; Cui, D.; Zhao, Z.; Kang, D.; Li, Z.; Albawardi, S.; Alsageer, S.; Alamri, F.; Alhazmi, A.; Amer, M.R.; et al. Highly sensitive, scalable, and rapid SARS-CoV-2 biosensor based on In(2)O(3) nanoribbon transistors and phosphatase. *Nano Res.* **2022**, *15*, 5510–5516. [[CrossRef](#)]
105. Ditte, K.; Nguyen Le, T.A.; Ditzer, O.; Sandoval Bojorquez, D.I.; Chae, S.; Bachmann, M.; Baraban, L.; Lissel, F. Rapid detection of SARS-CoV-2 antigens and antibodies using OFET biosensors based on a soft and stretchable semiconducting polymer. *ACS Biomater. Sci. Eng.* **2021**. [[CrossRef](#)]
106. Wu, Q.; Wu, W.; Chen, F.; Ren, P. Highly sensitive and selective surface plasmon resonance biosensor for the detection of SARS-CoV-2 spike S1 protein. *Analyst* **2022**, *147*, 2809–2818. [[CrossRef](#)]

**Disclaimer/Publisher’s Note:** The statements, opinions and data contained in all publications are solely those of the individual author(s) and contributor(s) and not of MDPI and/or the editor(s). MDPI and/or the editor(s) disclaim responsibility for any injury to people or property resulting from any ideas, methods, instructions or products referred to in the content.